Available online at www.sciencedirect.com

ScienceDirect

Thin Solid Films 515 (2006) 866–871

thin solid films

www.elsevier.com/locate/tsf

Property change in multifunctional TiC_xO_y thin films: Effect of the O/Ti ratio

A.C. Fernandes [a,*], P. Carvalho [a], F. Vaz [a], S. Lanceros-Méndez [a], A.V. Machado [b], N.M.G. Parreira [c], J.F. Pierson [d], N. Martin [e]

[a] *Universidade do Minho, Dept. Física, Campus de Azurém, 4800-058 Guimarães, Portugal*
[b] *Universidade do Minho, Dept. Eng. Polímeros, 4800-058 Guimarães, Portugal*
[c] *ICMES-Fac. Ciências Tecnologia Universidade de Coimbra, 3030-201 Coimbra, Portugal*
[d] *Laboratoire de Science et Génie des Surfaces (UMR CNRS 7570), Ecole de Mines, Parc de Saurupt, 54042 Nancy Cedex, France*
[e] *Laboratoire de Microanalyse des Surfaces, Ecole Nationale Supérieure de Mécanique et des Microtechniques, 25030 Besançon Cedex, France*

Available online 14 September 2006

Abstract

TiC_xO_y films with various O/Ti ratios have been deposited by DC magnetron sputtering, using C pieces incrusted in a Ti target erosion area. Composition analysis revealed the existence of three different growth regimes: (i) zone I, corresponding to films with metallic-like appearance, and atomic ratios O/Ti below one; (ii) zone II, with films revealing interference-like colours, and atomic ratios O/Ti higher than 2. Between these two regions, there was a transition zone T, where the atomic ratio O/Ti is between one and two. The films within this zone revealed a brown colour. X-ray diffraction (XRD) structural characterization results showed an evolution from a mixed Ti(C,O) phase at lower O/Ti ratio, to a quasi-amorphous structure within zone T, and poorly crystallized rutile and anatase TiO_2 at the highest O/Ti ratios (zone II). These different structural arrangements resulting from different film's compositions had clear effects on electrical resistivity, whose values increased from about 7×10^2 to 2×10^{11} μΩ cm with increase of the O/Ti ratio. Fourier-transform infrared spectroscopy (FTIR) was used to further confirm the different nature of films structure and, thus, to better understand their properties variation. The observed behaviour was found to be in straight correlation with those of XRD.

Keywords: Titanium oxycarbide; Sputtering; Structure; FTIR; Resistivity

1. Introduction

During the last 10 years, diamond-like carbon (DLC) films have been the subject of considerable interest, due to their special properties such as high hardness, low friction coefficients, high wear resistance, and chemical inertness. More recently, there have been several attempts to improve the properties of DLC films by the addition of other elements, such as silicon [1–3], nitrogen [4–6] and various metals [7–9].

Many modifications to DLC have been tried and the addition of, for example, nitrogen, to carbon films has been shown to reduce the inner stress, electrical resistivity and coefficient of friction [10,11]. In the same manner, oxygen has always been looked upon as an interesting element in thin film materials, not only because of its high reactivity with most metals, but also due to the changes that it induces in chemical bonding states and, thus, in the materials' electrical, optical and mechanical characteristics.

In order to expand our understanding of carbon-based thin films, the objective of the present research work is the preparation of one group of ceramic compounds based on the carbide binary system Ti–C. Transition-metal carbides such as TiC are very attractive materials due to their interesting mechanical and physical properties. They are characterized by high hardness and a high melting point [12], excellent electrical and thermal conductivity, high chemical and thermal stability, and good wear and corrosion resistance [13]. Due to this unique combination of properties, these materials have been extensively investigated and systematically used in many technological applications to improve significantly tool life [13]. Examples of this material used in microelectronics would include diffusion barriers and optical filters [14,15].

* Corresponding author. Tel.: +351 253510475; fax: +351 253510461.
E-mail address: acrist@fisica.uminho.pt (A.C. Fernandes).

0040-6090/$ - see front matter © 2006 Elsevier B.V. All rights reserved.
doi:10.1016/j.tsf.2006.07.047

In terms of chemical bonding, TiC exists not only in the stoichiometric form, but also in a substoichiometric form, with vacancies in the carbon lattice [16–18], and in overstoichiometric form, with an amorphous carbon tissue within grain boundaries [19,20]. Titanium carbide may have a minimum of 3% C vacancies in its fcc C sub-lattice and can have up to a maximum of 50% or even more vacancies and still retain its NaCl crystal structure [21]. This happens because it is a metastable structure; thus, both the metal and C atoms are located in fcc sub-lattices.

Following these basic material characteristics, it is expected that using small amounts of oxygen, especially in the substoichiometric TiC_x films ($x<1$), some changes in structure may occur and, thus, offer the possibility to tailor the material to a set of desired properties [22]. This idea is founded in the chemical inertness provided by oxides and the small atomic size of O; thereafter, it can be incorporated in substitution of C in the TiC_x compounds. Accordingly, the Ti(C,O) system seems to be a good candidate to the modern search for multifunctional materials. The presence of oxygen allows the tailoring of film properties between those of metallic-like carbides and those of the corresponding ionic oxides [22], allowing a wide range of possible applications. With this in mind, the emphasis of the present research work was on the structural changes in the films resulting from oxygen incorporation.

2. Experimental

The TiC_xO_y films were deposited by reactive dc magnetron sputtering, from a Ti target (200×100 mm^2) with 12 cylindrical C pieces (10 mm diameter) embedded in its erosion zone. Films were deposited onto single-crystal silicon wafers with (100) orientation and glass substrates, previously ultrasonically cleaned and sputter etched for 15 min in an Ar atmosphere (pressure of 0.15 Pa). The depositions were carried out in a laboratory-size deposition system. A gas atmosphere composed of $Ar+O_2$ was used. The Ar flow was kept constant at 60 sccm and the oxygen gas flow varied from 0 to 6 sccm (corresponding to a partial pressure variation between 0 and 5.1×10^{-2} Pa). The working pressure was approximately constant at 0.4 Pa and the substrates were grounded.

The atomic composition of the as-deposited samples was measured by electron probe microanalysis (EPMA) in a Cameca SX-50 apparatus. Ball crater tests were used to measure the thickness of the samples. The crystallographic structure was investigated by conventional $\theta/2\theta$ X-ray diffraction (XRD) in the Bragg–Brentano configuration, using monochromatic CuK_α radiation. The grain size was evaluated from analysis of X-ray diffraction line profiles fitted to Pearson VII functions. Electrical resistivity was deduced from sheet resistance measurements at room temperature, using the four point probe method following the Van der Pauw corrections. Infrared spectra were obtained in transmission mode on a Fourier Transformed Infrared (FTIR) Perkin Elmer 1600 spectrometer from 400 to 1600 cm^{-1}, using unpolarized light, with a resolution of 1 cm^{-1}.

3. Results and discussion

3.1. Composition and structure

Film thicknesses ranged from 1.5 to 6.3 μm and the Ti, O and C contents are plotted in Fig. 1 as a function of the oxygen flow. The plot also shows the variation of the O/Ti ratio as a function of the oxygen flow. This plot shows that O content increases almost linearly with the increase of the oxygen flow, while the Ti and C contents decrease. Particularly remarkable is the variation of the O/Ti ratio, which follows closely the O variation.

A deeper analysis to these results allows the possibility to divide the composition range into three distinct zones. The first zone, zone I, corresponds to films with a metallic-like appearance, revealing an atomic ratio O/Ti below one, with opposite tendencies for Ti and O variation. Ti concentration is reduced to about 1/3 of its initial value, while O increases about three times. The C content is also reduced, but only ~20%. In contrast to this first zone—a low O content one, there is another, referred in the text as zone II, where the O content is now dominant. The films within this zone have interference-like colours revealing an atomic ratio O/Ti higher than 2, which results in films close to stoichiometric TiO_2. In this region, the C content becomes negligible.

Between these two regions, results indicate the existence of a third region, noted in the text as a transition zone T, where the atomic ratio is between 1 and 2. The films within this zone have brown colour, similar to those observed by Bally et al. [23], when preparing TiO_{1+x} compounds.

The composition results are also well correlated with the structural features revealed by the XRD patterns, shown in Fig. 2. The figure shows the XRD patterns obtained for samples prepared within the different sputtering regimes, where the structural differences within each zone are evidenced. For comparison, a pure TiC_x film was also prepared (no oxygen gas flow, but using the same target current density as for the preparation of the Ti–C–O samples). The diffraction patterns shown in Fig. 2 reveal that this film exhibits reflections that might correspond to a mixture of two different phases: a hcp

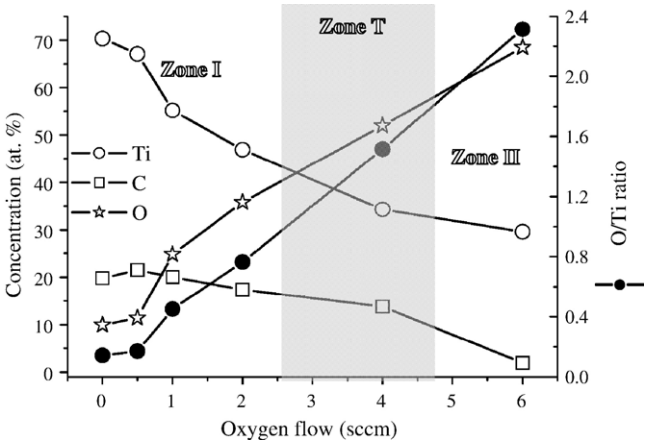

Fig. 1. Variation of the concentration of Ti, C and O (open symbols) and the ratio O/Ti (solid circles) as a function of the O_2 flow rate.

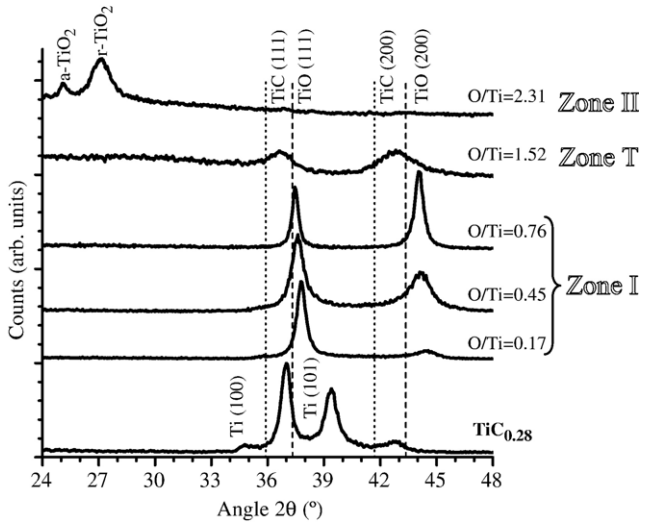

Fig. 2. $\theta/2\theta$ X-ray diffraction results (Cu K_α radiation), for the TiC_xO_y films.

metallic-like Ti and a fcc NaCl-type structure, whose nature cannot be clearly attributed. By composition analysis, it was found that the content of C was about 20 at.% and the one of Ti was close to 70 at.%. An amount of about 10 at.% O was also found in this sample, which might be the result of the residual atmosphere in the chamber [24,25], which may be simply incorporated within the matrix, leading to what might be called a Ti(C,O) solid solution. A shift towards lower angular positions was also observed in the peaks indexed to hcp Ti, which might be again the sign of interstitial inclusions of O and/or C.

The XRD patterns of films within zone I revealed the presence of only two diffraction peaks, whose indexation cannot be done without some doubts. The films have an almost constant C content, but with a substantial increase in the O amount. These films appear to have a rocksalt fcc-type structure, but since TiO and TiC are isomorphous phases, it is very difficult to unequivocally distinguish between which phase might act as a seed phase, or if in fact there is a mixture of both, forming a solid solution Ti(C,O)-type phase. In this zone, the films present more than 50 at.% Ti, which means that all these films should be substoichiometric (with lattice defects and distortions), inducing a shift in the diffraction peaks to higher angular positions. The evolution of the structure as a function of the O/Ti ratio in this zone I might be explained by the formation of a substoichiometric Ti(C,O) solid solution where, by the increase of the oxygen flow, the peaks shift progressively to lower diffraction angles very close to those fcc-TiO phase (ICDD card no. 77-2170), as a result of the lattice parameter increasing (oxygen insertion). This can be observed in Fig. 3, where the evolution of the TiO lattice parameter is plotted as a function of the O/Ti ratio. Films with an atomic ratio, O/Ti, below one have lattice parameters lower than those of the ICDD card, shifting to higher values when the atomic ratio is higher than 1.

Within the transition zone, results reveal a clear tendency to have quasi-amorphous films, as it can be evidenced in Fig. 2 by a significant peak broadening. In these films (illustrated by the film prepared at 4 sccm of O), the O/Ti ratio is already significantly high (around 1.5), but not enough to have TiO_2-type crystalline phases (anatase or/and rutile). This observation is consistent with the results of Bally et al. [23], which claimed that the films with this composition ratio should be amorphous. Martin et al. [26] reported that the TiO phase formation is restricted at high O concentrations due to the phase transition from TiO to TiO_2 (anatase or/and rutile), and thus, the relatively amorphous nature of the films in this region is expected.

Peak profiling in the XRD results from samples prepared within this transition region is difficult to accurately carry out, but probably these films present the formation of an over-stoichiometric Ti(C,O) solid solution.

For the highest oxygen flows, and following the already observed changes in composition depicted in Fig. 1, there is also another structural change, zone II, where a mixture of poorly crystallized rutile and anatase TiO_2 phases is evidenced. Composition measurements revealed an atomic ratio O/Ti of about 2.3, which is enough to ensure the formation of TiO_2 compounds since the atomic concentration of C is very low (below 5 at.%).

3.2. Influence of composition in bonding states characteristics

As the film's structure changes continuously from a solid solution Ti(C,O)-type structure within zone I towards a TiO_2 oxide-type structure (zone II), discontinuous changes as well as smooth and continuous ones are expected to be detected in the infrared spectra. This type of analysis is known as hard mode spectroscopy, in opposition to the analysis of directly involved modes, and it is a powerful method for the analysis of phase changes. Further, in this kind of mixed systems, the spectra are the consequence of both short- and long-range ordered regions and chemically ordered regions. Then, the selection rules are relaxed because of the disorder, off-center atomic shifts, presence of chemically ordered regions and/or local symmetry and the assignment of each mode becomes highly complex. This is why the observed broad peaks are rather labelled as bands, and only for the TiO_2 film (Fig. 4) the assignment of the well-known FTIR active modes is reported. Furthermore, and for

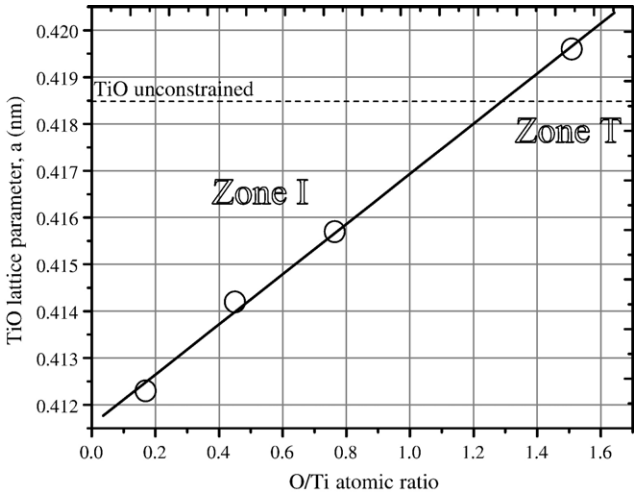

Fig. 3. Evolution of the lattice parameter of TiO phase as a function of the O/Ti ratio.

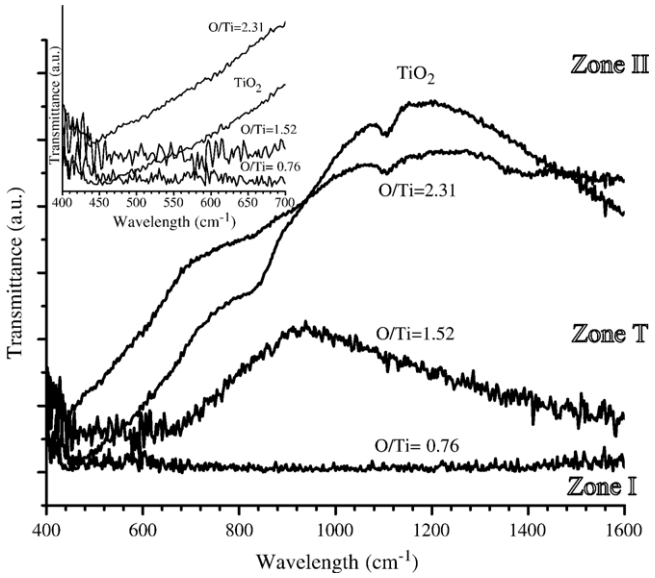

Fig. 4. Infrared spectra of TiC_xO_y films.

clarification purposes, the whole detailed analysis (intensity, line-width and frequency position) is not shown here, but rather the most pertinent features, which reveal/confirm the structural/chemical changes occurring at the films as the gas flow changes.

Fig. 4 shows the transmission spectra plotted in the range 400–1600 cm^{-1}. For comparison purposes, the result from a close stoichiometric oxide film (TiO_2) is also shown. As previously observed in the XRD characterization, the IR spectra also show that the results can be divided into three different types. The first group indexed to the referred zone I, is represented by the film with O/Ti=0.76, since there is no significant differences in the spectra from others with O/Ti<1. This fact is related with the metallic character of those films resulting in a very weak band around 400–500 cm^{-1}. This band is commonly attributed to the stretching of Ti–O–Ti bonds [27,28], which might be an indication of the TiO phase that was observed in XRD.

Again similar to XRD characterization, there are some changes in IR signals for films prepared with oxygen flow of 4 sccm (zone T). The upper left insert shows a detail of a region where films from zone II revealed a broad absorption band, and in fact, it is possible to conclude that for zone T films there are no significant absorption bands throughout the entire range. XRD results showed that this sample was quasi-amorphous and thus also in IR it is expected to see a significant broadening of absorption bands [29].

Regarding the results obtained for zone II films (including that reference TiO_2 film), it is worth to mention, first of all, the noticeable similarity between the oxycarbide sample (O/Ti ratio of 2.31) signal and that of "pure" TiO_2. This fact correlates again well with XRD results, which induced the existence of a mixed rutile/anatase TiO_2 phase-type for this oxycarbide sample. Moreover, one can distinguish (see upper left insert of Fig. 4) the presence of an absorption band centred around 440 cm^{-1}, which is known to be characteristic for TiO_2-type compounds [30]. At about 800 cm^{-1}, there is another absorption band, which is characteristic of the stretching of Ti–O bonds for the films presenting TiO_2 phases. A detailed analysis of the IR signal from the oxycarbide sample (O/Ti=2.31) also shows that there might be a very broad band between 1200 and 1400 cm^{-1}. Bibliographic data cannot accurately define its origin [29], but one possibility is that it may come from C–O bonds which may indicate there is some C inside the TiO_2 structure. This would be consistent with the fact that no signs of a TiC-type phase were detected by XRD. Furthermore, it is also important to notice the broad features around 1100 cm^{-1}, which are characteristic of oxide-type samples, but can also come from the Si–O bonds at the interfacial layer between film and substrate (Si in this case) [31], or even from some oxidation of substrate during film deposition (significant heating was observed in the high oxygen content samples).

3.3. Influence of composition on electrical behaviour

The evolution of the electrical resistivity in titanium oxycarbides is displayed in Fig. 5 as a function of the O/Ti atomic ratio, as well as the grain size deduced from XRD peak profiling, for films that presented the Ti(C,O) structure. Results show that electrical resistivity increases from about 7×10^2 to 2×10^{11} μΩ cm with an increase of the O/Ti ratio. In a more detailed analysis, this variation reveals again three distinct behaviours, in straight correlation with the composition and structural features. The first group includes the samples that were indexed to zone I, with resistivity values characteristic of metallic-like compounds, varying from 7×10^2 to 3×10^3 μΩ cm. These films have a high density of charge carriers and therefore present a relatively low electrical resistivity. This first zone is followed by an XRD quasi-amorphous phase, indexed as zone T, whose resistivity values show an increase in comparison to that of the zone I, for a value about 5×10^4 μΩ cm. The last region, indexed to a highly insulating-type TiO_2 phase mixture by XRD, has consequently much higher resistivity values, around 10^{11}–10^{12} μΩ cm.

In order to understand this behaviour, one must keep in mind that material resistivity is a complex phenomena, mainly

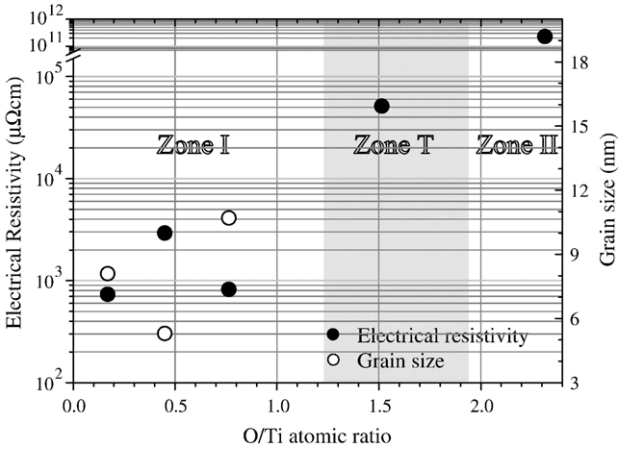

Fig. 5. Electrical resistivity at room temperature (293 K) and grain size from XRD patterns as a function of the O/Ti ratio.

determined by the intrinsic properties, defects and temperature. In this sense, by varying the O content and performing experiments at room temperature, resistivity (or conductivity) values will be particularly sensitive to phase composition variations, structure/microstructure and defects (dislocations, impurities and grain boundaries become determinant parameters) [21]. In this respect, the observed tendency to amorphization (increase of grain boundaries) observed in the films within the transition zone induce an increase in electron reflection coefficient at the grain boundaries and thus increasing the film's resistivity.

According to this factor, it is worth mentioning that the electrical properties of films are commonly analysed and known to be grain size-dependent and there are at least two phenomena that may contribute to that behaviour: first, the size-dependent nature of grain boundary segregation, and second, the defect thermodynamics at grain boundaries [32]. As can be observed in Fig. 5 and for the particular case of samples from zone I (where structural features seem quite similar), the resistivity values follow the evolution of grain size, as already observed by other authors [33–35].

For the samples within zone I, the main parameter that might explain the relatively low values is related to the roughly metallic nature of both TiC and TiO phases [36,37]. In both cases, the two Ti-4s valence electrons that are involved in conductivity of the pure metal are redistributed in the compounds: approximately 1/2 transferred to C and O-2p orbitals, and 1/2 move into unfilled Ti-3d orbitals [38]. Thus, TiC and TiO have no band gap at E_F (Fermi level) and, therefore, are not insulators/semiconductors, but metallic electronic conductors [21].

4. Conclusions

TiC_xO_y thin films were deposited by dc reactive magnetron sputtering from a Ti target with some embedded C pieces. The results showed that the evolution of film properties may be separated into three different growth regimes that developed. Composition analysis revealed that these three different growth regimes are characterized by different O/Ti ratios. Zone I corresponds to films with metallic-like appearance, and atomic ratios O/Ti below one. Zone II showed films with interference-like tones, and atomic ratios O/Ti higher than 2. Between these two regions, there is a transition zone T, where the atomic ratio is also higher than one. The films within this zone have brown colour.

These different composition results have clear influence on the type of structures that were formed and seems to evolve from a substoichiometric fcc Ti(O,C) solid solution at lower O/Ti ratios, to a quasi-amorphous structure, that might be an over-stoichiometric fcc Ti(O,C) solid solution in the transition zone and finally to poorly crystallized rutile and anatase TiO_2 at the highest O/Ti ratios. These different structural arrangements were further confirmed by Infrared Absorption Spectroscopy data, which revealed a strong relationship between the structural evolution and chemical changes.

Electrical resistivity testing showed a significant increase of resistivity values with increasing oxygen flow, which means the development of more insulating-type films. Measured values ranged from about 7×10^2 (roughly metallic) to 2×10^{11} μΩ cm (tending to insulating-type behaviour) with an increase of the O/Ti ratio. The evolution was found to be again closely related to structural changes. Similar behaviour was also observed in FTIR, reinforcing the different nature of the films.

Acknowledgements

The authors gratefully acknowledge the financial support of the Portuguese FCT institution by Project No. POCTI/38086/CTM/2001 co-financed by European Community Fund FEDER.

References

[1] A.A. Ogwu, R.W. Lamberton, S. Morley, P. Maguire, J. McLaughlin, Physica, B + C 269 (1999) 335.
[2] S. Camargo, R. Santos, A. Neto, R. Carius, F. Finger, Thin Solid Films 332 (1998) 130.
[3] K. Lee, M. Kim, S. Cho, K. Eun, T. Seong, Thin Solid Films 308–309 (1997) 263.
[4] S. Bhattacharyya, C. Cardinaud, G. Turban, J. Appl. Phys. 83 (1998) 4491.
[5] F.L. Freire Jr., D.F. Franceschini, Thin Solid Films 293 (1997) 236.
[6] A. Bousetta, M. Lu, A. Bensaoula, J. Vac. Sci. Technol., A, Vac. Surf. Films 13 (1995) 1639.
[7] C.P. Klages, R. Memming, Mat. Sci. Forum 52–53 (1989) 609.
[8] M. Wang, K. Schmidt, K. Reichelt, H. Dimigen, Hubsch, J. Mater. Res. 7 (1992) 667.
[9] M. Grischke, K. Bewilogua, H. Dimigen, Mater. Manuf. Process. 8 (1993) 407.
[10] H. Dimigen, C.P. Klages, Surf. Coat. Technol. 49 (1991) 543.
[11] D. Monaghan, D. Teer, P. Logan, I. Efeoglu, R. Arnell, Surf. Coat. Technol. 60 (1993) 525.
[12] E.L. Toth, Transition Metal Carbides and Nitrides, Academic Press, New York, 1971.
[13] A. Zaoui, S. Kacimi, B. Bouhafs, A. Roula, Physica, B + C 358 (2005) 63.
[14] G. Soto, Appl. Surf. Sci. 230 (2004) 254.
[15] F. Santerre, M.A. El Khakani, M. Chaker, J.P. Dodelet, Appl. Surf. Sci. 148 (1999) 24.
[16] K.E. Tan, A.M. Bratkovsky, R.M. Harris, A.P. Horsfield, D. Nguyen-Manh, D.G. Pettifor, A.P. Sutton, Model. Simul. Mater. Sci. Eng. 5 (1997) 187.
[17] A. Mani, P. Aubert, F. Mercier, H. Khodja, C. Berthier, P. Houdy, Surf. Coat. Tecnhol. 194 (2005) 190.
[18] S. Jhi, S.G. Louie, M.L. Cohen, J. Ihm, Phys. Rev. Lett. 86 (2001) 15.
[19] A. Czyzniewski, W. Precht, J. Mater. Process. Technol. 157–158 (2004) 274.
[20] W. Prencht, A. Czyzniewski, Surf. Coat. Technol. 174–175 (2003) 979.
[21] W. Williams, Int. J. Refract. Met. Hard Mater. 17 (1999) 21.
[22] A.C. Fernandes, F. Vaz, L. Rebouta, A. Pinto, E. Alves, N.M.G. Parreira, Ph. Goudeau, E. Le Bourhis, J.P. Rivière, Surf. Coat. Technol. (in press).
[23] A.R. Bally, P. Hones, R. Sanjinés, P.E. Schmid, F. Lévy, Surf. Coat. Technol. 108–109 (1998) 166.
[24] M. Audronis, P.J. Kelly, R.D. Arnell, A. Leyland, A. Matthews, Surf. Coat. Technol. 200 (2005) 1616.
[25] D.C. Reigada, R. Prioli, L.G. Jacobsohn, F.L. Freire Jr., Diamond Relat. Mater. 9 (2000) 489.
[26] N. Martin, O. Banakh, A.M.E. Santo, S. Springer, R. Sanjinés, J. Takadoum, F. Lévy, Appl. Surf. Sci. 185 (2001) 123.
[27] M. Nakamura, L. Sirghi, T. Aoki, Y. Hatanaka, Surf. Sci. 507–510 (2002) 778.
[28] N. Phonthammachai, T. Chairassameeong, E. Gulari, A.M. Jamieson, S. Wongkasemjit, Microporous Mesoporous Mater. 66 (2003) 261.
[29] N. Cruz, E.C. Rangel, M.H. Tabacknics, B.C. Trasferretti, C.U. Davanzo, Nucl. Instrum. Methods., B 175–177 (2001) 721.

[30] V.G. Erkov, S.F. Devyatova, E.L. Molodstova, T.V. Malsteva, U.A. Yanovskii, Appl. Surf. Sci. 166 (2000) 51.
[31] G. He, Q. Fang, J.X. Zhang, L.Q. Zhu, M. Liu, L.D. Zhang, Nanotechnology 16 (2005) 1641.
[32] C. Demetry, X. Shi, Solid State Ionics 118 (1999) 271.
[33] R.B. Kale, C.D. Lokhande, Appl. Surf. Sci. 223 (2004) 343.
[34] H. Chen, Y. Lu, W. Hwang, Thin Solid Films 49 (2006) 266.
[35] V. Baranauskas, T. Santos, M. Schreiner, Z. Jingguo, A. Mammana, C. Mammana, Sens. Actuators, B, Chem. 85 (2002) 90.
[36] O. Banakh, P.E. Schmid, R. Sanjinés, F. Lévy, Surf. Coat. Technol. 151–152 (2002) 272.
[37] C. Leumg, M. Weinert, P. Allen, R. Wentzcovitch, Phys. Ver., B 54 (1996) 7857.
[38] V.A. Gubanov, A.L. Ivanosvsky, V.P. Zhukov, Electronic Structure of Refractory Carbides and Nitrides, Cambridge University Press, Cambridge, 1994.